

Pattern Formation of Spin-Polarized Fermions in a Fast Rotating Boson-Fermion Mixture

Rina Kanamoto and Makoto Tsubota

Department of Physics, Osaka City University, Osaka 558-8585, Japan

(Dated: December 2, 2024)

By minimizing the coupled mean-field energy functionals, we investigate the properties of a rotating atomic boson-fermion mixture in a two-dimensional parabolic trap. At low angular frequencies, the semiclassical Thomas-Fermi approximation with the rigid-body rotation is confirmed to be valid for fermions. At high angular frequencies, the system enters a regime where quantized vortices form in the bosonic condensate, and a finite number of degenerate fermions form the maximum-density-droplet state for a weak boson-fermion coupling. We find that as the coupling constant increases, the maximum density droplet develops into a lower-density state reflecting the symmetry of the vortex lattice, and then reconstructs an edge-like state, thus revealing characteristics of a Landau-level structure.

PACS numbers: 03.75.Hh, 03.75.Lm, 03.75.Ss

Experimental developments in the cooling techniques of atomic gases have provided new opportunities to investigate the quantum-degenerate regime where Bose-Einstein (BE) condensations, Fermi-Dirac (FD) degeneracies [1, 2], and BE condensations of paired states emerge [3, 4]. Recently the heteronuclear Feshbach resonance was found in a boson-fermion mixture [5], and has opened a new field of unique quantum-statistical phenomena. This system sheds light not only on our understanding of boson-mediated pairing of fermions [6], but also on the relationship to condensed matter physics [7], multicomponent systems [8], and the study of the normal and superfluid states of fermions [9].

When a superfluid system is subjected to a rotation above a critical angular frequency, the system forms quantized vortices, which are observed both in bosonic [10] and fermionic [11] systems. On the other hand, a number of analogies have been pointed out between the states of neutral atoms subjected to a rotation and charged particles in a magnetic field [12, 13]. For instance, the Laughlin wave function in the fractional or integer quantum hall state can describe wave functions for bosons with a number of quantized vortices [14, 15] as well as wave functions for degenerate fermions under a fast rotating drive. Another example is that a finite number of electrons in a quantum dot (QD) (e.g., realized in a semiconductor heterostructure) form the maximum density droplet (MDD) state [16], reflecting the Landau-level structure of electrons under a strong magnetic field. In the MDD, the total angular momentum of electrons takes the lowest possible value due to the FD degeneracy and the Pauli exclusion principle. However, the interplay between the Pauli pressure plus potential term and the electron-electron interaction causes an instability against density modulation or edge reconstruction [17, 18].

In this Letter, we show that a finite number of spin-polarized fermions in a boson-fermion mixture under rotation form a family of density patterns. In particular,

as the boson-fermion coupling increases, the system goes through the following patterns: an atomic MDD, broken-symmetry states associated with the vortex lattice in a bosonic condensate, and an edge-like state in the phase-separating regime. These density patterns clearly show how level crossing of the single-particle energy occurs, and how the fermi gas acquires the angular momentum in the ground state.

We consider the gaseous atomic system of N_B bosons and spin-polarized N_F fermions in a rotating two-dimensional (2D) parabolic trap. The trapping frequencies and atomic masses for the two components are assumed to be identical, being denoted as ω and M . Throughout this paper, the angular momenta, energies, and lengths are measured in units of \hbar , $\hbar\omega$, $l = \sqrt{\hbar/(M\omega)}$, respectively. We include boson-boson and boson-fermion s -wave interactions within the mean-field approximation, assuming the weak couplings between atoms and neglecting correlations. Let us suppose that the bosonic atoms are BE-condensed and described by a condensate wave function ψ_B , whereas the fermionic atoms are FD-degenerate and have single-particle orbitals $\psi_F^{(j=1,\dots,N_F)}$. The mean-field energy functional in the rotating frame is given by

$$E_B = N_B \int d^2r \psi_B^*(\mathbf{r}) \left[\hat{H} + \frac{g}{2} n_B(\mathbf{r}) \right] \psi_B(\mathbf{r}), \quad (1)$$

$$E_F = \sum_{j=1}^{N_F} \varepsilon_F^{(j)}; \quad \varepsilon_F^{(j)} = \int d^2r \psi_F^{(j)*}(\mathbf{r}) \hat{H} \psi_F^{(j)}(\mathbf{r}), \quad (2)$$

$$E_{BF} = h \int d^2r n_F(\mathbf{r}) n_B(\mathbf{r}), \quad (3)$$

where $\hat{H} = (-\nabla^2 + r^2)/2 - \Omega \hat{L}_z$ is the Hamiltonian for a free atom with the angular-momentum operator $\hat{L}_z = -i(x\partial_y - y\partial_x)$, and the 2D boson-boson and boson-fermion couplings are denoted as $g(\geq 0)$ and $h(\geq 0)$, respectively. The (conditional) densities are given by $n_B(\mathbf{r}) = N_B |\psi^{(B)}(\mathbf{r})|^2$, and $n_F(\mathbf{r}) = \sum_{j=\text{occ}} |\psi_F^{(j)}(\mathbf{r})|^2$,

where the summation over j is taken over all occupied states. The eigensolutions of \hat{H} are given by

$$\varepsilon_{nm}^{(0)} = n + m + 1 - \Omega(m - n), \quad n, m = 0, 1, \dots, \quad (4)$$

$$u_{nm}(\mathbf{r}) = \frac{1}{\sqrt{\pi n! m!}} e^{\frac{r^2}{2}} (\partial_x + i\partial_y)^m (\partial_x - i\partial_y)^n e^{-r^2}, \quad (5)$$

which are well-defined angular momentum states, i.e., $\hat{L}_z u_{nm}(\mathbf{r}) = (m - n)u_{nm}(\mathbf{r})$. To obtain the ground states of both components self-consistently, we expand the single-particle orbitals as $\psi_B(\mathbf{r}) = \sum_{n,m} b_{nm} u_{nm}(\mathbf{r})$, and $\psi_F^{(j)}(\mathbf{r}) = \sum_{n,m} f_{nm}^{(j)} u_{nm}(\mathbf{r})$ with the normalization conditions $\sum_{n,m} b_{nm}^2 = \sum_{n,m} f_{nm}^{(j)2} = 1$, where b_{nm} and $f_{nm}^{(j)}$ are taken to be real without loss of generality. We then numerically iterate minimization of $\tilde{\varepsilon}_B = (E_B + E_{BF})/N_B$ and diagonalization of $\tilde{\varepsilon}_F = \varepsilon_F + h \int d^2r \psi_F^* n_B \psi_F$ until a self-consistent convergence [19, 20]. Because we use a mean-field approximation, the rotational symmetry of the condensate is spontaneously broken by the vortex-lattice formation, which also causes symmetry breaking in the fermionic cloud due to the boson-fermion coupling.

The single-particle energy of a fermion $\tilde{\varepsilon}_F$ in the presence of the boson-fermion interaction is modified from that of a free fermion as shown in Fig. 1 (a), where thick and thin lines correspond to the occupied and unoccupied levels. At $\Omega = 0$, the degeneracies in $\varepsilon_{nm}^{(0)}$ with respect to $n + m$ are partially lifted according to the angular momentum $|m - n|$. The single-particle energy increases relative to the noninteracting value when h is positive and decreases when h is negative, and the amount of the deviation from $\varepsilon_{nm}^{(0)}$ at $\Omega = 0$ is maintained until a vortex forms in the condensate. The boson-fermion coupling

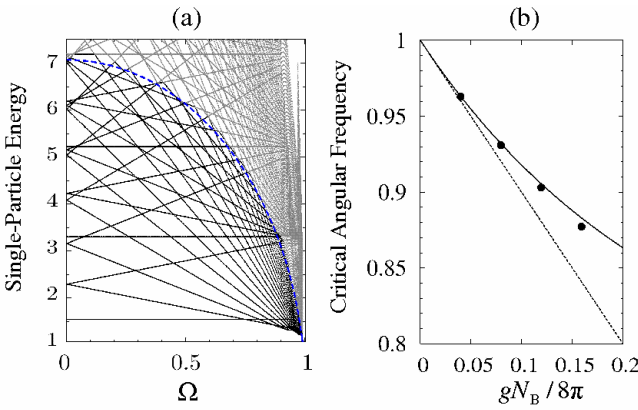


FIG. 1: (a) Single-particle energy of fermions $\tilde{\varepsilon}_F$ weakly interacting with bosonic condensate for $N_B = 1000$, $N_F = 25$, and $g = 0.5h = 2 \times 10^{-3}$. Dashed curve is the chemical potential given by the Thomas-Fermi theory for free fermions. (b) Critical angular frequency of single-vortex formation in the condensate for $N_B = 1000$. Solid and dotted curves correspond to analytic results Ω_{cr} and $\Omega_{cr}^{(LLL)}$, respectively. Filled circles show the numerical results including the effect of the boson-fermion interaction with $h = g$.

only affects a few fermions near the bottom of the Fermi sea because the boson-fermion interaction conserves angular momentum where the bosons are condensed in the zero angular-momentum state.

We compare the mean-field results with those obtained by the semiclassical Thomas-Fermi (TF) theory with the assumption of rigid-body rotation. The 2D TF energy functional for fermions [21] is given by

$$E^{TF} = \int d\mathbf{r} \left[\pi n_F^2(\mathbf{r}) + \frac{r^2}{2} (1 - \Omega^2) n_F(\mathbf{r}) + h n_B(\mathbf{r}) n_F(\mathbf{r}) \right], \quad (6)$$

where the first term corresponds to the kinetic contribution $\sum_{k \leq k_F} \mathbf{k}^2$ with the local fermi wave number determined by $n_F(\mathbf{r}) = \pi k_F^2(\mathbf{r})/(2\pi)^2$, the second term is the effective trapping potential including centrifugal effect, and the third term is the boson-fermion interaction. For a slow rotation, the third term is insignificant compared to the first and second ones; therefore, we neglect the third term as a first approximation. The radius of the fermionic cloud and density distribution are then obtained as $R_F = [8N_F/(1 - \Omega^2)]^{1/4}$, and $n_F(\mathbf{r}) = (1 - \Omega^2)(R_F^2 - r^2)/(4\pi)$, respectively. The chemical potential is determined so that the integration of density over space equals to N_F , as $\mu_F = \sqrt{2N_F(1 - \Omega^2)}$. The value of μ_F decreases with an increase of Ω , and is in good agreement with the fermi energy obtained numerically [Fig. 1 (a)] in the slow rotation regime.

The critical angular frequency of the single-vortex formation in the bosonic condensate is determined by the condition that the energy of the condensate with a vortex equals that without vortex. To determine this frequency, we simplify the system by neglecting the boson-fermion interaction and then analytically minimize E_B . Within the lowest-Landau-level (LLL) approximation, the condensate without vortex is characterized by $b_{00} = 1$, and that with a vortex is characterized by $b_{01} = 1$. The critical angular frequency is hence obtained as $\Omega_{cr}^{(LLL)} = 1 - G$ where $G \equiv gN_B/(8\pi)$. However, when the higher Landau level with $n = 1$ is included, the energy of the no vortex state is minimized by the occupation $b_{11}^2 = G^2/(8G^2 + 2G + 1)$ and $b_{00}^2 = 1 - b_{11}^2$. For the single-vortex state, the contribution of the $(n, m) = (1, 2)$ state is almost negligible. As a result, the critical value for the case including the higher-Landau level is $\Omega_{cr} = 1 - G - 2b_{11}^2 - 2Gb_{11}[b_{11} - (1 + b_{00}^2)b_{00}]$. We compare the numerical results, which includes the effects of boson-fermion interaction, with the above two analytical results in Fig. 1 (b). The figure shows that the effect of higher Landau level becomes significant for larger boson-boson coupling, but it also shows that the boson-fermion interaction has little effect on the critical angular frequency. Furthermore, we numerically confirmed that the effect of the higher-Landau levels are negligible for $\Omega \gtrsim \Omega_{cr}$ for the weak coupling cases that we used throughout the calculations.

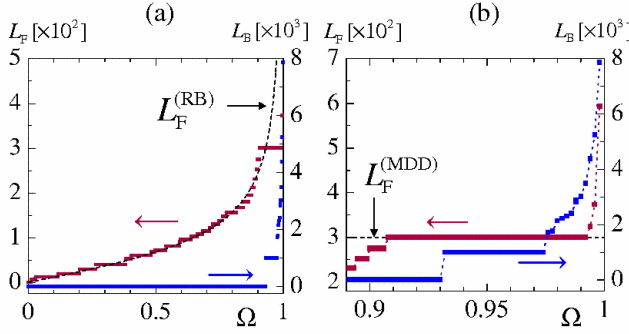


FIG. 2: Total angular momentum of each component. (a) Large steps in L_B arise from the irrotationality and formation of quantized vortices. Small steps in L_F arise from the size effect, but these steps are smeared-out for larger $N_F (\gtrsim 500)$. Dashed curve corresponds to the angular momentum of rigid-body rotation $L_F^{(RB)}$ of free fermions. (b) Enlargement of the fast rotating regime in (a). The horizontal dashed line corresponds to $L_F^{(MDD)}$.

The total angular momentum of each component is shown in Fig. 2 (a) as a function of Ω . For the bosonic condensate, $L_B = N_B \sum_{n,m} b_{nm}^2 (m - n)$ remains zero due to the superfluidity, and jumps to N_B at Ω_{cr} . In contrast, the total angular momentum of fermions $L_F = \sum_{j=\text{occ}} \sum_{n,m} f_{nm}^{(j)2} (m - n)$ increases when Ω exceeds 0. The summation L_F is well approximated by the function $L_F^{(RB)} = \Omega \int r^2 n_F(\mathbf{r}) d^2\mathbf{r} = (8N_F)^{3/2} \Omega / (24\sqrt{1 - \Omega^2})$, which is the angular momentum for the rigid-body rotation of free fermions [Fig. 2 (a), dashed curve]. In the slow rotating regime, the semiclassical TF theory for a free fermi gas is therefore confirmed to be a good description of the fermions [22] coupled with the bosons.

In the fast rotating regime, in which quantized vortices successively form in the bosonic condensate, the semiclassical TF theory for fermions fails because of the significance of interaction effects and the quantized nature arises from the finite size. This is shown by the results in Fig. 2 (b). The total angular momentum of the fermions L_F becomes frozen at the value $L_F^{(MDD)} = N_F(N_F - 1)/2$ when the degenerate fermions occupy the lowest level $m = 0$ up to the highest level $m = N_F - 1$ in the LLL whereas $L_F^{(RB)}$ diverges. At this value $L_F^{(MDD)}$, the density n_F is maximum, and this state is called the MDD for QDs with a finite number of electrons [16].

The many-body wave function of fermions is given by the Slater determinant constructed from the single-particle orbitals $\psi_F^{(j)}$. The many-body wave function of the MDD state, constructed by $\psi_F^{(j)}(\mathbf{r}) = u_{0m}(\mathbf{r})$ for $0 \leq m \leq N_F - 1$, is shown to be the Laughlin wave function of the integer quantum hall state of $\nu = 1$ with the use of Vandermonde formula. We find that this state exists for the range $0.91 \lesssim \Omega \lesssim 0.99$, even in the presence of the boson-fermion interaction. However, as shown in

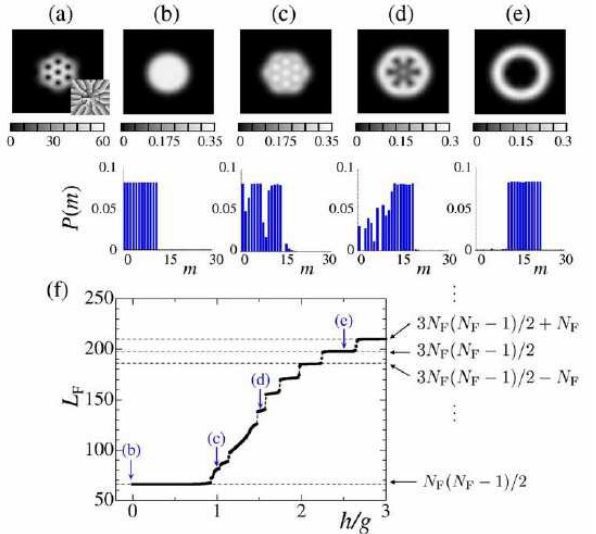


FIG. 3: (a) Density and phase profile of the bosonic condensate wave function. (b)-(e) Density profiles and mean angular-momentum distributions $P(m)$ of the fermionic cloud for $h/g = 0, 1, 1.5$, and 2.5 , respectively. (f) Total angular momentum of fermions.

Fig. 2 (b), L_F again increases in the limit $\Omega \rightarrow 1$, which indicates that the interplay between the energy scale of interaction and the level spacings leads to a reconstruction of the ground state with a higher angular momentum. In the boson-fermion mixture, in contrast to the electronic system with the interparticle Coulomb interaction, it is the boson-fermion interaction that causes the ground-state reconstruction in a fermi gas, where a small boson-fermion coupling affects fermions up to the fermi energy due to degeneracies in this limit.

To examine how the boson-fermion coupling modulates the MDD state in the fast rotating regime, we restrict the bases u_{nm} within the LLL $n = 0$, and increase h while keeping the other parameters fixed ($\Omega = 0.995$, $N_B = 1000$, $N_F = 12$, and $g = 2 \times 10^{-3}$). The density and phase profile of the condensate wave function is nearly independent of h for the given values of the fixed parameters, and looks like ones shown in Fig. 3 (a). In the condensate, seven singly-quantized vortices form the Abrikosov lattice characterized by the 2π branch cuts in the phase profile. This bosonic density works as a robust effective potential for the fermions. In contrast, the fermionic density n_F is sensitive to the increase in h . The changing density profiles are shown in the upper panels of Fig. 3 (b)-(e). The histograms show the mean angular-momentum distribution in the fermionic cloud defined by $P(m) \equiv \sum_{j=\text{occ}} |f_{0m}^{(j)}|^2 / N_F$. In the MDD state [(b)], the angular-momentum distribution is given by $1/N_F$ for $0 \leq m \leq N_F - 1$. When the weak interaction is introduced [(c)], the occupations of some low-angular-momentum states are partially shifted to higher-angular-momentum states, which are not occupied in the MDD

state. The fermionic density increases in the vortex cores of the condensate, breaking the rotational symmetry in order to reduce the repulsive interaction energy. As h increases further [(d)], more angular-momentum states are shifted, and the region where bosons and fermions overlap gradually decreases. The bosonic and fermionic densities eventually separate [23] for larger value of h [(e)], where a large central hole emerges in the fermionic cloud. The mean angular-momentum distribution becomes almost uniformly equal to $1/N_F$ for $M \leq m \leq M + N_F - 1$. The rotational symmetry in n_F is again recovered independent of the configuration of the vortex lattice in the bosonic condensate. Such a quasi-1D-like density and corresponding angular-momentum distribution also occur in the case of free fermions in $\Omega \gtrsim 1$ with an elimination of the centrifugal singularity [12, 24].

In Fig. 3 (f), we show the change in the total angular momentum of fermions L_F when the ground-state reconstruction occurs. For a weak coupling $h/g \lesssim 1$, $L_F \simeq L_F^{(\text{MDD})}$ because an increase in L_F costs the potential and kinetic energies than the interaction energy. However, L_F gradually increases in order to reduce the interaction energy for $1 \lesssim h/g \lesssim 1.5$ where the rotational symmetry of n_F is broken. When the phase separation occurs for $h/g \gtrsim 1.5$, L_F is quantized associated with the fact that the fermi gas recovers the rotational symmetry where $P(m)$ becomes almost constant as in Fig. 3 (e). After the overlap of the two components disappears, the jumps in L_F is given by $\sum_{m=M+1}^{M+N_F} m - \sum_{m=M}^{M+N_F-1} m = N_F$, i.e., the quantization of L_F arises from the process that the occupied lowest-angular-momentum state $m = M$ is shifted to the unoccupied lowest-angular-momentum-state $m = M + N_F$. For the state in Fig. 3 (e), interestingly, L_F is almost equivalent to $3L_F^{(\text{MDD})}$.

In conclusion, we have found the unique behaviors of spin-polarized fermions coupled with the BE condensate in the fast rotating regime. We expect that an experimental observation of the angular momentum will provide clear evidence of the Landau-level structure of both components under rotation, and these results help stimulate studies of integer and fractional quantum hall states of atoms with different quantum statistics. We acknowledge Akira Oguri for fruitful discussion and comments.

[1] A.G. Truscott, K.E. Strecker, W.I. McAlexander, G.B. Partridge, and R.G. Hulet, *Science*, **291**, 2570 (2001); F. Schreck, L. Khaykovich, K.L. Corwin, G. Ferrari, T. Bourdel, J. Cubizolles, and C. Salomon, *Phys. Rev. Lett.* **87**, 080403 (2001).

[2] B. DeMarco and D.S. Jin, *Science* **285**, 1703 (1999).

[3] E.A. Donley, N.R. Claussen, S.T. Thompson, and C.E. Wieman, *Nature (London)* **417**, 529 (2002).

[4] K.M. O'Hara, S.L. Hemmer, M.E. Gehm, S.R. Granade, J.E. Thomas, *Science* **298**, 2179 (2002); C.A. Regal, C. Ticknor, J.L. Bohn, and D.S. Jin, *Nature (London)* **424**, 47 (2003).

[5] S. Inouye, J. Goldwin, M.L. Olsen, C. Ticknor, J.L. Bohn, and D.S. Jin, *Phys. Rev. Lett.* **93**, 183201 (2004).

[6] M.J. Bijlsma, B.A. Heringa, and H.T.C. Stoof, *Phys. Rev. A* **61**, 053601 (2000); J. Tempere, V.N. Gladilin, I.F. Silvera, and J.T. Devreese, *Phys. Rev. B* **72**, 094506 (2005).

[7] L. Mathey, D.-W. Wang, W. Hofstetter, M.D. Lukin, and E. Demler, *Phys. Rev. Lett.* **93**, 120404 (2004); M. Cramer, J. Eisert, F. Illuminati, *Phys. Rev. Lett.* **93**, 190405 (2004); T. Miyakawa, H. Yabu, and T. Suzuki, *Phys. Rev. A* **70**, 013612 (2004); M. Salerno, e-print cond-mat/0503097.

[8] C. Ospelkaus, S. Ospelkaus, K. Sengstock, and K. Bongs, e-print cond-mat/0507219; T. Karpiuk, M. Brewczyk, S. Ospelkaus-Schwarzer, K. Bongs, M. Gajda, and K. Rzażewski, *Phys. Rev. Lett.* **93**, 100401 (2004).

[9] A. Minguzzi and M.P. Tosi, *Phys. Rev. A* **63**, 023609 (2001); C.P. Search, H. Pu, W. Zhang, and P. Meystre, *Phys. Rev. A* **65**, 063615 (2002); M. Cozzini and S. Stringari, *Phys. Rev. Lett.* **91**, 070401 (2004); G. Tonini and Y. Castin, e-print cond-mat/0504612.

[10] K.W. Madison, F. Chevy, W. Wohlleben, and J. Dalibard, *Phys. Rev. Lett.* **84**, 806 (2000); J.R. Abo-Shaeer, C. Raman, J.M. Vogels, W. Ketterle, *Science* **292**, 476 (2001).

[11] M.W. Zwierlein, J.R. Abo-Shaeer, A. Schirotzek, C.H. Schunck, and W. Ketterle, *Nature (London)* **435**, 1047 (2005).

[12] T.-L. Ho and C.V. Ciobanu, *Phys. Rev. Lett.* **85**, 4648 (2000).

[13] M. Toreblad, M. Borgh, M. Koskinen, M. Manninen, and S.M. Reimann, *Phys. Rev. Lett.* **93**, 090407 (2004).

[14] R.B. Laughlin, *Phys. Rev. B* **27**, 3383 (1983); *ibid* *Phys. Rev. Lett.* **50**, 1395 (1983).

[15] N.K. Wilkin and J.M.F. Gunn, *Phys. Rev. Lett.* **84**, 6 (2000).

[16] A.H. MacDonald, S.R.E. Yang, and M.D. Johnson, *Aust. J. Phys.* **46**, 345 (1993).

[17] S.M. Reimann, M. Koskinen, M. Manninen, and B.R. Mottelson, *Phys. Rev. Lett.* **83**, 3270 (1999).

[18] C. de C. Chamon and X.G. Wen, *Phys. Rev. B* **49**, 8227 (1994).

[19] D.A. Butts and D.S. Rokhsar, *Nature (London)* **397**, 327 (1999); G.M. Kavoulakis, B. Mottelson, and C.J. Pethick, *Phys. Rev. A* **62**, 063605 (2000).

[20] T. Karpiuk, M. Brewczyk, and K. Rzażewski, *Phys. Rev. A* **69**, 043603 (2004).

[21] S. Ghosh, M.V.N. Murthy, and S. Sinha, *Phys. Rev. A* **64**, 053603 (2001).

[22] D.A. Butts and D.S. Rokhsar, *Phys. Rev. A* **55**, 4346 (1997).

[23] K. Mølmer, *Phys. Rev. Lett.* **80**, 1804 (1998); R. Roth and H. Feldmeier, *Phys. Rev. A* **65** 021603(R) (2002); L. Viverit, C.J. Pethick, and H. Smith, *Phys. Rev. A* **61**, 053605 (2000).

[24] A.L. Fetter, *Phys. Rev. A* **64**, 063608 (2001); E. Lundh, *Phys. Rev. A* **65**, 043604 (2002); K. Kasamatsu, M. Tsubota, and M. Ueda, *Phys. Rev. A* **66**, 053606 (2002); V. Bretin, S. Stock, Y. Seurin, and J. Dalibard, *Phys. Rev. Lett.* **92**, 050403 (2004).